Available online at www.sciencedirect.com
SCIENCE DIRECT
Chemical Physics Letters 424 (2006) 358–363
CHEMICAL PHYSICS LETTERS
www.elsevier.com/locate/cplett

Luminescence properties of sol–gel derived spherical $SiO_2@Gd_2(WO_4)_3:Eu^{3+}$ particles with core–shell structure

P.Y. Jia [a,b], X.M. Liu [a,b], M. Yu [a], Y. Luo [a,b], J. Fang [c], J. Lin [a,*]

[a] Key Laboratory of Rare Earth Chemistry and Physics, Changchun Institute of Applied Chemistry, Chinese Academy of Sciences, Changchun 130022, PR China

[b] Graduate School of the Chinese Academy of Sciences, Beijing 100049, PR China

[c] Department of Chemistry and Advanced Materials Research Institute, University of New Orleans, New Orleans, LA 70148, USA

Received 14 February 2006; in final form 18 April 2006
Available online 30 April 2006

Abstract

Monodisperse, core–shell structured $SiO_2@Gd_2(WO_4)_3:Eu^{3+}$ particles were prepared by the sol–gel method. The samples were characterized by X-ray diffraction (XRD), field emission scanning electron microscopy, transmission electron microscopy, photoluminescence (PL) and low-voltage cathodoluminescence (CL). PL and CL study revealed that the core–shell structured $SiO_2@Gd_2(WO_4)_3:Eu^{3+}$ particles show strong red emission dominated by the $^5D_0$–$^7F_2$ transition of Eu^{3+} at 615 nm with a lifetime of 0.89 ms. The PL and CL emission intensity can be tuned by the coating number of $Gd_2(WO_4)_3:Eu^{3+}$ phosphor layers on SiO_2 particles, the size of the SiO_2 core particles, and by accelerating voltage and the filament current, respectively.

1. Introduction

Recently, considerable efforts have been devoted to the design and preparation of composite particles consisting of core covered by shells of different chemical composition. The interests in such core–shell materials stem from the fact that the properties (mechanical, optical, electrical, magnetic and catalytic) of core or shell can be tailored by their size, morphology, component and structure of their shells or cores [1–3]. A great number of processes have been developed to prepare core–shell materials, such as template-directed self-assembly [4], precipitation and surface reaction [5], layer-by-layer technique [6] and sonochemical method [7].

The current demand for high-resolution, high brightness and high efficiency in phosphors for cathode ray tubes, field emissive displays and plasma display panel has promoted the development of phosphors. Particularly, phosphors with nonagglomerated, monodisperse, spherical (<2 μm) morphology are of great interest, because they offer higher packing density, lower scattering of light, brighter luminescent performance, higher definition, and more improved screen packing density [8,9]. Nowadays, many synthetic routes have been developed to control the size, morphology and distribution of phosphor particles, such as spray pyrolysis [10] and fluxes precipitation [11], but it is still difficult to obtain highly monodisperse spherical phosphor particles from these processes.

It is well known that monodisperse spherical silica particles from nano- to submicron range can be prepared by hydrolysis and condensation of tetraethoxysilane (TEOS) catalyzed by ammonia [12]. If the silica spheres are coated with layers of phosphors, a kind of core–shell phosphor materials with spherical morphology will be obtained, and the size for the phosphor particles can be controlled by the silica cores. Furthermore, because silica is cheaper than most of the phosphor materials (which often employ the expensive rare earth elements as the activators and/or

* Corresponding author. Address: Key Laboratory of Rare Earth Chemistry and Physics, Changchun Institute of Applied Chemistry, Chinese Academy of Sciences, 5625 Renmin Street, Changchun 130022, PR China.
E-mail address: jlin@ciac.jl.cn (J. Lin).

0009-2614/$ - see front matter © 2006 Elsevier B.V. All rights reserved.
doi:10.1016/j.cplett.2006.04.088

host components), the core–shell phosphor materials will be cheaper than the pure phosphor materials in unit mass. $RE_2(WO_4)_3$ ($RE = La^{3+}$, Ce^{3+}, Pr^{3+}, Nd^{3+}, Sm^{3+}, Eu^{3+}, Gd^{3+}, Tb^{3+}, Dy^{3+}, Ho^{3+}) has been widely investigated for its prominent luminescent properties, among which $Gd_2(WO_4)_3$ is an important phosphor host material [13–15]. Accordingly, in the present work we prepared monodisperse core–shell structured $SiO_2@Gd_2(WO_4)_3:Eu^{3+}$ via the sol–gel process and investigate their photoluminescent and cathodoluminescent properties.

2. Experimental section

Amorphous sub-micrometer silica spheres with size ranging from 400 to 700 nm were synthesized by the well-known Stöber process, i.e., the hydrolysis and condensation of tetraethoxysilane (TEOS) in an ethanol solution containing water and ammonia, as described previously [12,16]. $SiO_2@Gd_2(WO_4)_3:Eu^{3+}$ core–shell phosphors were prepared by a Pechini sol–gel process [15,17]. The doping concentration of Eu^{3+} is 30 mol% of Gd^{3+} in $Gd_2(WO_4)_3$ host, which had been optimized previously [15]. Stoichiometrically, 0.5068 g Gd_2O_3 (99.99%, Shanghai Yuelong New Materials Co. Ltd.), 0.2112 g Eu_2O_3 (99.99%, Shanghai Yuelong New Materials Co. Ltd.), were dissolved in dilute HNO_3 (analytical reagent, AR) under vigorous stirring, and the superfluous HNO_3 was driven off until the pH value of the solution between two and three. The above solution was mixed with 1.6500 g ammonium (meta) tungstate hydrate ($H_{26}N_6O_{41}W_{12} \cdot 18H_2O$ (Fluka), 20 mL water–ethanol (V/V = 15: 5) solution containing citric acid (AR) as a chelating agent for the metal ions. The molar ratio of metal ions to citric acid was 1:2. As a cross-linking agent, polyethylene glycol (PEG, molecular weight = 10000, AR) was added with a final concentration of 0.20 g/mL. The final solution was stirred for 1 h to form a sol, and then the silica particles were added under stirring. The suspension was further stirred for another 4 h, and then the silica particles were separated by centrifugation. The samples were dried at 100 °C for 1 h immediately. Then the dried samples were annealed to 500 °C with a heating rate of 1 °C/min and held there for 2 h in air. The above process was repeated for three times to increase the thickness of the $Gd_2(WO_4)_3:Eu^{3+}$ shells. After these processes, the sample was annealed to 800 °C with a heating rate of 5 °C/min, and hold there for 2 h in air. In this way, the core–shell structured $SiO_2@Gd_{1.4}Eu_{0.6}(WO_4)_3$ samples were been obtained. For the purpose of comparison, the coating sol was evaporated in an 80 °C water bath to form gel, which was annealed in a similar process to produce the pure $Gd_{1.4}Eu_{0.6}(WO_4)_3$ powder.

The X-ray diffraction (XRD) of samples were examined on a Rigaku-Dmax 2500 diffractometer using Cu Kα radiation ($\lambda = 0.15405$ nm). The morphology of samples was inspected using a field emission scanning election microscope (FESEM, XL30, Philips), transmission electron microscope (TEM, JEOL-2010, 200 kV). The photoluminescence (PL) excitation, emission spectra and cathodoluminescence (CL) spectra were taken on a Hitachi F-4500 spectrofluorimeter equipped with a 150 W xenon lamp and a self-made electron gun (10^{-6} Pa vacuum, 1000–5000 V) as the excitation source, respectively. The luminescence decay curve was measured on a Lecroy Wave Runner 6100 Digital Oscilloscope (1 GHz) using 266 nm laser (pulse width = 4 ns) using YAG: Nd as the excitation source. All the measurements were performed at room temperature.

3. Results and discussion

3.1. Formation and morphology of core–shell particles

The formation and morphology of the core–shell particles have been examined by XRD, FESEM and TEM, respectively. Fig. 1 shows the XRD patterns of 800 °C annealed bare SiO_2 (a), $Gd_{1.4}Eu_{0.6}(WO_4)_3$ (b) and $SiO_2@Gd_{1.4}Eu_{0.6}(WO_4)_3$ (c) particles as well as the standard data for $Gd_2(WO_4)_3$ (JCPDS No. 23-1076) (d) as a reference, respectively. For SiO_2 particles annealed at 800 °C (Fig. 1a), no diffraction peak is observed except for a broad band centered at $2\theta = 22.0°$, which is the characteristic peak for amorphous SiO_2 (JCPDS 29-0085). For the $SiO_2@Gd_{1.4}Eu_{0.6}(WO_4)_3$ core–shell sample fired at 800 °C (Fig. 1b), besides the broad band at $2\theta = 22.0°$ from amorphous SiO_2, all the diffraction peaks belonging to crystalline $Gd_2(WO_4)_3$ are present, suggesting that the coatings of $Gd_{1.4}Eu_{0.6}(WO_4)_3$ have crystallized well on the surfaces of amorphous silica particles. This coincides well with the XRD pattern of pure $Gd_{1.4}Eu_{0.6}(WO_4)_3$ particles annealed at 800 °C (Fig. 1c) and the standard data for $Gd_2(WO_4)_3$ (JCPDS No. 23-1076). No other phase has been detected, indicating that no reaction occurred between the SiO_2 cores and $Gd_{1.4}Eu_{0.6}(WO_4)_3$ shells. In general, the nanocrystallite size can be estimated from the Scherrer

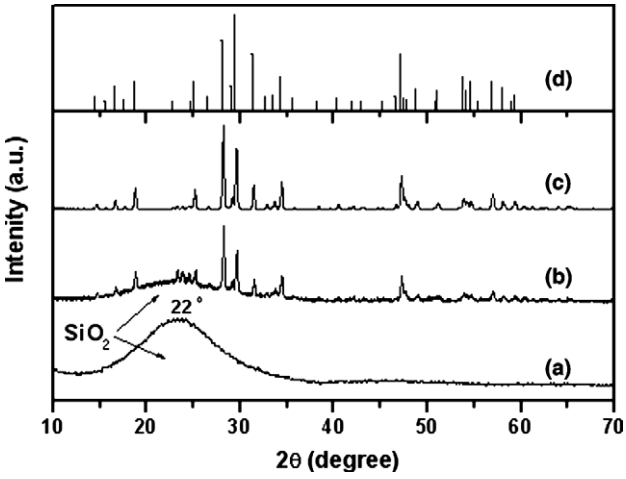

Fig. 1. XRD patterns of SiO_2 (a), $SiO_2@Gd_{1.4}Eu_{0.6}(WO_4)_3$ (b) and $Gd_{1.4}Eu_{0.6}(WO_4)_3$ (c) samples annealed at 800 °C as well as the standard data for $Gd_2(WO_4)_3$ (JCPDS No.72-0257) (d) as a reference.

formula: $D_{hkl} = K\lambda/(\beta\cos\theta)$, where λ is the X-ray wavelength (0.15405 nm), β is the full-width at half-maximum, θ is the diffraction angle, K is a constant (0.89) and D_{hkl} means the size along (hkl) planes [18]. The estimated crystallite size is around 20 nm.

Fig. 2 shows the FESEM micrographs of the bare SiO_2 (a, b, c, d) and the corresponding $SiO_2@Gd_{1.4}Eu_{0.6}(WO_4)_3$ (a1, b1, c1, d1, four times coated) core–shell particles annealed at 800 °C, respectively. The bare SiO_2 samples consist of nonaggregated, monodisperse and spherical particles with size of 400 nm (Fig. 2a), 500 nm (Fig. 2b), 600 nm (Fig. 2c) and 700 nm (Fig. 2d), respectively. After functionalizing the SiO_2 particles with $Gd_{1.4}Eu_{0.6}(WO_4)_3$ coatings, the resulting $SiO_2@Gd_{1.4}Eu_{0.6}(WO_4)_3$ particles still keep the morphology of the silica core particles, i.e., these particles are still nonagglomerated, monodisperse and spherical, as shown in Fig. 2a1–d1, respectively. However, due to the additional layers of $Gd_{1.4}Eu_{0.6}(WO_4)_3$ coated on SiO_2 particles, the $SiO_2@Gd_{1.4}Eu_{0.6}(WO_4)_3$ particles become not as smooth as the corresponding bare silica ones, and have sizes of 500 nm (Fig. 2a1), 600 nm (Fig. 2b1), 700 nm (Fig. 2c1) and 800 nm (Fig. 2d1) (i.e., about 100 nm larger than the corresponding the bare silica ones), respectively.

TEM was performed to verify the core–shell structure of $SiO_2@Gd_{1.4}Eu_{0.6}(WO_4)_3$ particles directly. As a representative example, the TEM micrographs of 400 nm – SiO_2 bare spheres and those coated (four times) with $Gd_{1.4}Eu_{0.6}(WO_4)_3$ layers are shown in Fig. 3a and b, respectively. Only black spheres (400 nm in diameter) were observed for bare SiO_2 particles (Fig. 3a). In contrast, the core–shell structure for the $SiO_2@Gd_{1.4}Eu_{0.6}WO_4$ particles

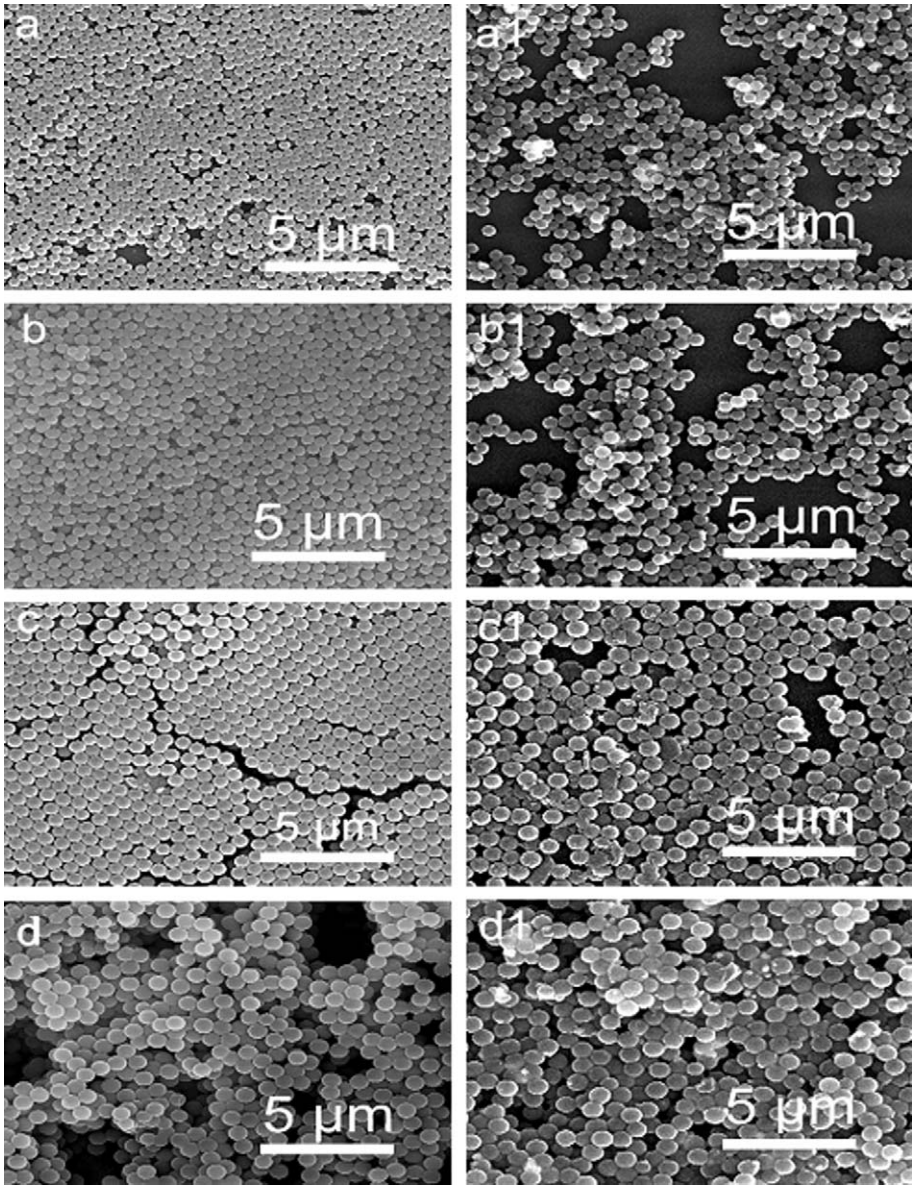

Fig. 2. FESEM micrographs amorphous SiO_2 particles with different sizes before (a, b, c, d) and after (a1, b1, c1, d1) coating with $Gd_{1.4}Eu_{0.6}(WO_4)_3$ layers annealed at 800 °C.

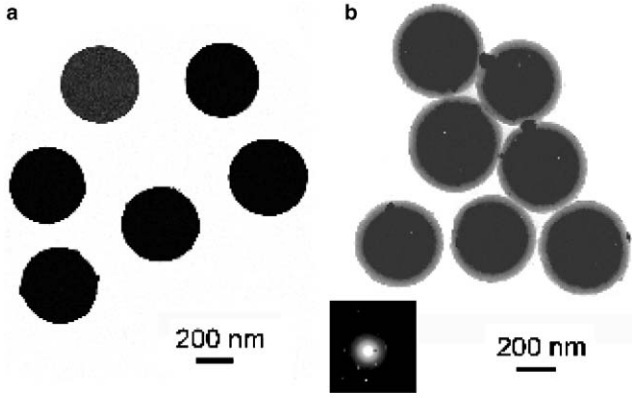

Fig. 3. TEM micrographs of bare SiO_2 (a) and core–shell structured $SiO_2@Gd_{1.4}Eu_{0.6}(WO_4)_3$ (b) particles annealed at 800 °C.

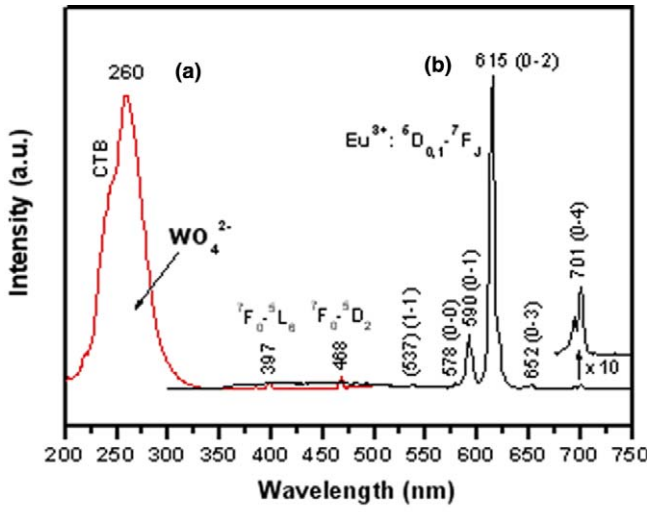

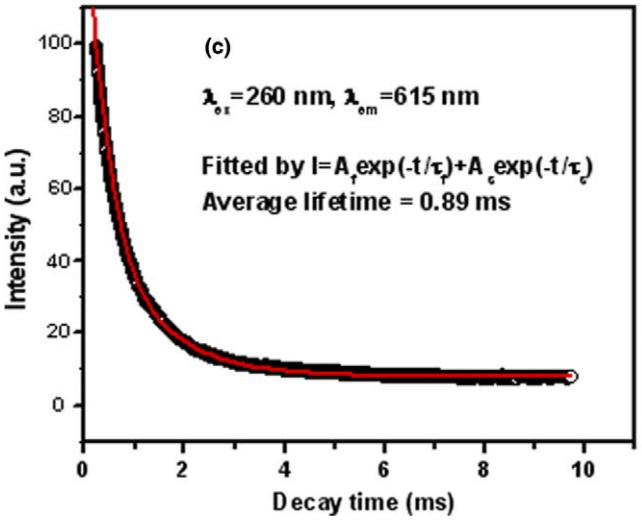

Fig. 4. Excitation (a), emission (b) spectra and decay curve (c) of Eu^{3+} in core–shell structured $SiO_2@Gd_{1.4}Eu_{0.6}(WO_4)_3$ sample annealed at 800 °C.

(Fig. 3b) can be seen clearly due to the different electron penetrability for the cores and shells. The cores are black spheres with an average size of 400 nm (similar to the pure SiO_2 particles in Fig. 3a), and the shells have gray color with an average thickness of 50 nm. The electron diffraction measurement performed in the interface region of the core and shell of a particle (inset of Fig. 3b) has shown electron diffraction rings with some disorder, just demonstrating the coexistence of crystalline phase [$Gd_{1.4}Eu_{0.6}(WO_4)_3$] and amorphous phase (SiO_2) in the interface region of the core–shell particle.

At last, we would like to elucidate the formation process of the core–shell structured $SiO_2@Gd_{1.4}Eu_{0.6}WO_4$ particles qualitatively. In the Pechini process, the citric acid first formed chelates with Gd^{3+} and Eu^{3+} ions, then the left carboxylic acid groups in the citric acid reacted with polyethylene glycol to form polyester with a suitable viscosity. The Stöber process-derived silica particles contained large amount of free hydroxyl groups (–OH) and silanol groups (Si–OH) on their surface [19]. By stirring silica particles in the solution, a lot of Gd^{3+}, Eu^{3+} and tungstate groups were absorbed onto the silica particles by physical and chemical interactions. After drying and annealing process, these species reacted and crystallized on the surface of SiO_2 particles, resulting in the formation of $SiO_2@Gd_{1.4}Eu_{0.6}WO_4$ core–shell particles. These particles are very stable for a long time.

3.2. Luminescence properties

Under ultraviolet radiation, $SiO_2@Gd_{1.4}Eu_{0.6}(WO_4)_3$ core–shell phosphor particles show red emission. Fig. 4 shows the excitation (a) and emission (b) spectra as well as the decay curve of Eu^{3+} in of $SiO_2@Gd_{1.4}Eu_{0.6}(WO_4)_3$ sample. Monitored by the $^5D_0$–$^7F_2$ transition of Eu^{3+} at 615 nm, the obtained excitation spectrum consists of a broad band peaking at 260 nm with a shoulder at 240 nm and a group of sharp peaks originating from Eu^{3+} f–f transitions (397 nm: $^7F_0$–$^5L_6$; 468 nm: $^7F_0$–$^5D_2$). The broad band at 260 nm is due to W^{6+}–O^{2-} charge transfer transition and the shoulder peak at 240 nm may be ascribed to the Eu^{3+}–O^{2-} charge transfer transition [14,15]. The presence of WO_4^{2-} absorption in the excitation spectrum of Eu^{3+} indicates that there exists an energy transfer from WO_4^{2-} to Eu^{3+} in the sample [14,15]. Excitation into WO_4^{2-} at 260 nm yields the characteristic emission of Eu^{3+} (Fig. 4b), which contains the characteristic emission from the excited $^5D_{0,1}$ to ^7F_J ($J = 0$–4) of Eu^{3+}, with $^5D_0$–$^7F_2$ hypersensitive forced electric-dipole transition being the most prominent group. This is because the Eu^{3+} ions occupy the Gd^{3+} sites (C_{nv} symmetry, without inversion center) in $Gd_2(WO_4)_3$ host [14]. The $^5D_0$–$^7F_4$ (around 700 nm) of Eu^{3+}, which belongs to forced electric-dipole transition, should also be present with a comparable intensity in this case. However, in Fig. 4 it is present with a very weak intensity (which can be seen clearly by enlarging by 10 times). This situation might be caused by the low sensitivity of our photomultiplier's response around 700 nm. Note that the $^5D_0$–$^7F_0$ transition of Eu^{3+}

shows one peak at 578 nm, suggesting the existence of only one kind Eu^{3+} site in the host lattices [20].

The PL decay curve for Eu^{3+} in $SiO_2@Gd_{1.4}Eu_{0.6}(WO_4)_3$ is shown Fig. 4c, which can not be fitted into a single exponential function, but a double exponential function as $I = A_f\exp(-t/\tau_f) + A_s\exp(-t/\tau_s)$ (τ_f and τ_s are the fast and slow components of the luminescence lifetimes, A_f and A_s are the fitting parameters, respectively). The average lifetime for Eu^{3+} can be determined by the formula as $\tau = (A_f\tau_f^2 + A_s\tau_s^2)/(A_f\tau_s + A_f\tau_s)$ [21], and the average lifetimes for Eu^{3+} in $SiO_2@Gd_{1.4}Eu_{0.6}(WO_4)_3$ is determined to be 0.89 ms. The double exponential decay behavior of the activator (Eu^{3+}) is frequently observed when the excitation energy is transferred from the donor (WO_4^{2-}) [21].

It is interesting to note that the PL intensity of the $SiO_2@Gd_{1.4}Eu_{0.6}(WO_4)_3$ core–shell structured phosphors can be tuned by the SiO_2 core particle size and the coating number of $Gd_{1.4}Eu_{0.6}(WO_4)_3$ phosphor shells. Table 1 lists the PL intensity of the $SiO_2@Gd_{1.4}Eu_{0.6}(WO_4)_3$ sample as a function of the SiO_2 core particle size and the coating number (N). Clearly seen form the figure, the PL intensity increases with the increase of SiO_2 core particle size and coating numbers. In general, bigger phosphor particle size is good for the improvement of the PL intensity of phosphors [8]. Here, it is believed that the amount of emitting Eu^{3+} ions per SiO_2 particle will increase with the increase of SiO_2 cores, resulting in the enhancement of the PL intensity. Similarly, with the increase of coating number, the thickness of $Gd_{1.4}Eu_{0.6}(WO_4)_3$ shell will increase accordingly, thus leading to the increase of the PL intensity.

Similar to the emission under UV light illumination, the $SiO_2@Gd_{1.4}Eu_{0.6}(WO_4)_3$ core–shell particles also exhibit strong red emission under the excitation of electron beam. The CL emission spectrum under the excitation of electron beam (5 kV) is similar to the PL emission spectrum (Fig. 4b). The CL intensity of $SiO_2@Gd_{1.4}Eu_{0.6}(WO_4)_3$ has been investigated as a function of accelerating voltage and the anode (filament) current, and the results are shown in Table 2. It can be seen clearly from Table 2 that the CL intensity increases with the increase of accelerating voltage (1–5 kV) and anode current (14–18 mA). With the increase of accelerating voltage and anode current, more plasmas will be produced by the incident electrons, resulting more Eu^{3+} ions being excited and thus higher CL intensity. Due to the strong low voltage CL intensity and excellent dispersing properties of $SiO_2@Gd_{1.4}Eu_{0.6}(WO_4)_3$ core–shell phosphors, they are potentially applied in field emission display (FED) devices.

Table 1
PL intensity of $SiO_2@Gd_{1.4}Eu_{0.6}(WO_4)_3$ samples as a function of SiO_2 particle size and coating number

SiO_2 core (nm)	400	500	600	700
PL intensity (a.u.)	62687	65140	87714	99875
Coating number (N)	1	2	3	4
PL intensity (a.u.)	54798	76833	96032	99875

Table 2
CL emission intensity of $SiO_2@Gd_{1.4}Eu_{0.6}(WO_4)_3$ core–shell structured sample as a function of accelerating voltage and anode current

Voltage (kV)	1	2	3	4	5
CL intensity (a.u.)	8995	10650	11739	12508	12973
Current (mA)	14	15	16	17	18
CL intensity (a.u.)	13666	15808	20859	31175	60133

4. Conclusions

A simple and effective sol–gel process has been developed to coat $Gd_2WO_4)_3$:Eu^{3+} phosphor layers on monodisperse and spherical SiO_2 particles with different sizes. The obtained core–shell structured $SiO_2@Gd_2WO_4)_3$:Eu^{3+} phosphors maintain spherical morphology and narrow size distribution. Under UV light and low-voltage electron beam excitation, the $SiO_2@Gd_2WO_4)_3$:Eu^{3+} phosphors show the characteristic red emission of Eu^{3+} (dominated by $^5D_0$–$^7F_2$ transition at 615 nm). The PL intensity increases with the increase of coating number and the size of SiO_2 particles. This provides effective ways to tune the PL intensity of the phosphors. The CL intensity also increases with the increase of anode current and accelerating voltage, leading the core–shell phosphors to have potential application in FED devices.

Acknowledgments

This project is financially supported by the foundation of 'Bairen Jihua' of Chinese Academy of Sciences, the National Natural Science Foundation of China (50225205, 50572103 and 20431030) and the MOST of China (No. 2003CB314707). Dr. M. Yu is grateful for the special starting research fund for the Awardees of President Prize of Chinese Academy of Sciences (2005–2007). Prof. J. Fang is grateful for the financial support by the foundation of a two-base program for international cooperation of NSFC (00310530) related to Project 50225205, and NSF DMR-0449580.

References

[1] Q. Liu, Z. Xu, J.A. Finch, R. Egerton, Chem. Mater. 10 (1998) 3936.
[2] S.M. Verónica, S. Marina, F. Michael, Adv. Funct. Mater. 15 (2005) 1036.
[3] F. Caruso, Adv. Mater. 13 (2001) 11.
[4] S.M. Marinakos, J.P. Novak, L.C. Brousseau, A.B. House, E.M. Edecki, J.C. Feldhaus, D.L. Feldheim, J. Am. Chem. Soc. 1321 (1999) 8518.
[5] M. Ohmori, E. Matijevic, J. Colloid Interf. Sci. 160 (1993) 288.
[6] P. Schuetzand, F. Caruso, Chem. Mater. 14 (2002) 4509.
[7] Z. Zhong, M. Yitzhak, K. Yuri, Y. Zhao, A. Gedanken, Chem. Mater. 11 (1999) 2350.
[8] X. Jing, T.G. Ireland, C. Gibbons, D.J. Barber, J. Silver, A. Vecht, G. Fern, P. Trogwa, D. Morton, J. Electrochem. Soc. 146 (1999) 4546.
[9] Y.D. Jiang, Z.L. Wang, F. Zhang, H.G. Paris, C.J. Summers, J. Mater. Res. 13 (1998) 2950.
[10] S.H. Cho, J.S. Yoo, J.D. Lee, J. Electrochem. Soc. 145 (1998) 1017.
[11] A. Celikkaya, M. Akinc, J. Am. Ceram. Soc. 73 (1990) 2360.
[12] W. Stöber, A. Fink, E. Bohn, J. Colloid Interf. Sci. 26 (1968) 62.

[13] K. Nassau, H.J. Levinstein, G.M. Loiacono, J. Am. Ceram. Soc. 47 (1964) 363.
[14] C.A. Kodaira, H.F. Brito, M.C.F.C. Felinto, J. Solid State Chem. 171 (2003) 401.
[15] M.L. Pang, J. Lin, M. Yu, J. Solid State Chem. 177 (2004) 2237.
[16] G.H. Bogush, M.A. Tracy, C.F. Zukoski, J. Non-cryst. Solids 104 (1988) 95.
[17] M.P. Pechini, U.S. Patent 3 330 697, 1967.
[18] L.S. Birks, H. Friedman, J. Appl. Phys. 17 (1946) 687.
[19] Y. Chen, J.O. Iroh, Chem. Mater. 11 (1999) 1218.
[20] G. Blasse, B.C. Grabmaier, Luminescent Materials, Springer, Berlin/Heidelberg, 1994.
[21] T. Fujii, K. Kodaira, O. Kawauchi, N. Tanaka, H. Yamashita, M. Anpo, J. Phys. Chem. B 101 (1997) 10631.